Journal of Alloys and Compounds 708 (2017) 380–384

Contents lists available at ScienceDirect

Journal of Alloys and Compounds

journal homepage: http://www.elsevier.com/locate/jalcom

# *In situ* TEM tensile testing on high-entropy alloy coating by laser surface alloying

Zhaobing Cai [a], Xiufang Cui [a, **], Guo Jin [a, *], Binwen Lu [a], Danli Zhang [b], Zhanming Zhang [b]

[a] Institute of Surface/Interface Science and Technology, Key Laboratory of Superlight Material and Surface Technology of Ministry of Education, College of Material Science and Chemical Engineering, Harbin Engineering University, Harbin 150001, China
[b] Center for Advancing Materials Performance from the Nanoscale (CAMP-Nano) & Hysitron Applied Research Center in China (HARCC), State Key Laboratory for Mechanical Behavior of Materials, Xi'an Jiaotong University, Xi'an 710049, China

ARTICLE INFO

*Article history:*
Received 14 December 2016
Received in revised form
21 February 2017
Accepted 5 March 2017
Available online 7 March 2017

*Keywords:*
*In situ* TEM
Tensile
Fracture
High-entropy alloy coating
Laser surface alloying

ABSTRACT

A unique technique, *in situ* TEM tensile testing, was used to investigate the fracture process of Ni-Cr-Co-Ti-V-Al high-entropy alloy coating with complex phases. The results of *in situ* TEM observation indicated that during the fracture process, dislocations get together in the interface between BCC HEA phase and (Co, Ni)$Ti_2$ compounds and crack propagation happens along the phase interface, leading to the final rupture, which proves that the phase interface may be the probable failure place. Also, the fracture strength and Young's modulus were calculated according to the stress-strain curve from the *in situ* TEM tensile testing. The stress-strain curve shows a good linearity, confirming the brittle failure. The fracture strength is calculated to be ~3.3 GPa and the fracture strain is measured to be ~3.1%. The Young's modulus of the tensile sample is calculated to be ~102 GPa, quite close to that of bulk titanium alloy.



## 1. Introduction

Tensile property is one of the most important mechanical properties of materials for many design applications. In general, for structural materials or bulk materials, macro tensile testing is the best way to evaluate the tensile property [1–5]. In our knowledge, engineering stress-engineering strain curve and fracture morphology are the most studied aspects of macro tensile testing. However, during macro tensile testing, the formation of defects such as dislocation, the extension of cracks and the evolution of fracture are also our concerns. So a new method, *in situ* observation especially by a transmission electron microscope (TEM), arises at the historic moment [6–18]. Until now, there have been some studies about nano-scaled materials tested inside a TEM, for example, single-crystal alloy (Au [19], Ni [7–9], Mo [10] and a-Ti [11]), thin films [12,13] and metallic glasses [14–16]. All in all, these previous studies are focused on the mechanical behaviors of materials with relatively simple structure (BCC, FCC, HCP single-crystal or amorphous) [17]. For materials with complex phases, there are basically no studies about *in situ* observation by TEM.

High-entropy alloy (HEA), proposed by Yeh et al., is becoming a burgeoning and frontier scientific research field [20,21]. The current studies about high-entropy alloy are mainly paid attention to their structure characterization, properties characterization and phase formation rules while researches of microscopic mechanism are relatively less. In this regard, advances in characterization should be applied to comprehensively understand the properties of HEAs such as fracture [22]. Recently, some advanced characterization techniques about *in situ* observation have been applied, that is, *in situ* neutron diffraction study [23] and *in situ* TEM straining experiment [24]. Yet, these objects for *in situ* observation are also simple HEAs with single solid solution structure. Fortunately, they provide new ideas to study HEAs from the micro-scale even nano-scale. In the present study, we attempt to observe the whole fracture process of high-entropy alloy coating with complex phases at the nanoscale using *in situ* TEM tensile testing. By recorded movie of tensile testing, the fracture process was displayed clearly. Nanoscale origin of fracture for HEA coating, coming from phase interface, was identified.

Supplementary video related to this article can be found at

* Corresponding author. 145, Nantong Ave, Nangang Distinct, Harbin, Heilongjiang 150001, China.
** Corresponding author. 145, Nantong Ave, Nangang Distinct, Harbin, Heilongjiang 150001, China.
*E-mail addresses:* cuixf721@163.com (X. Cui), jinjg721@163.com (G. Jin).

http://dx.doi.org/10.1016/j.jallcom.2017.03.049
0925-8388/

http://dx.doi.org/10.1016/j.jallcom.2017.03.049.

## 2. Experimental methods

Ni-Cr-Co-Ti-V-Al HEA coating was synthesized by laser surface alloying, as described previously [25] and recapped here in brief. By ball-milling, premixed powder, containing pure elemental powder Ni, Cr, Co and V, was pre-placed onto the surface of Ti-6Al-4V substrate, using ethyl alcohol as binders. A laser system (YLS-3000, IPG, Germany) was used to form Ni-Cr-Co-Ti-V-Al HEA coating and the parameters of laser surface alloying were: laser power of 2000W, laser spot diameter of 3 mm and laser speeding of 40 mm/s. Then the HEA coating was utilized to prepare the sample for *in situ* TEM tensile testing, shown in Fig. 1. First, the HEA coating was cut to the size of 3 mm × 3 mm × 1 mm using wire-cut electric discharge machine. Samples were then ground manually with SiC papers down to a thickness of ~100μm. After that, samples were corroded by the solution of 4% HF + 4% $HNO_3$ + 92% $H_2O$, and put on the surface of tailored copper table for the next process of focused ion beam (FIB, FEI Nova 200 Nano Lab-dual beam, Netherlands) to produce electron-transparent and specific regions for observation during *in situ* TEM tensile testing with the ion beam at 5pA/30 KV. Afterwards, the samples were transferred to the device of *in situ* TEM tensile testing and tungsten trip was utilized to fasten the T-shaped free end of tensile sample.

The *in situ* TEM tensile testing were conducted at room temperature with a Hysitron PI95 TEM PicoIndenter® in a JEOL 2100 field emission gun TEM (JEOL, Japan) operating at 200 KV. The stand-alone tensile sample with a tungsten grip assembly was shown in the last TEM image of Fig. 1. Fig. 1 also displays the assembly drawing of overall tensile testing and the yellow arrow showed the force direction of *in situ* TEM tensile testing. The average strain rate of *in situ* TEM tensile testing was $2 \times 10^{-3}$ $s^{-1}$ and the movie of this tensile was recorded by a Gatan CCD camera. In addition, a method of finite element modelling was used to study the stress distribution with the help of a software of ABAQUS. The model of finite element modelling is set up in brief according to the real distribution of BCC HEA phase and (Co, Ni)$Ti_2$ phase in the *in situ* TEM tensile testing shown in Fig. 3 and the schematic diagram of tensile testing is displayed in Fig. 5.

## 3. Results and discussion

The HEA coating used for *in situ* TEM tensile testing was mainly composed of a B2 HEA phase and (Co, Ni)$Ti_2$ compounds (FCC) [25] shown in Fig. 2a. Fig. 2b gives the intuitive evidence to prove the complex coating containing two phases, namely, HEA phase and (Co, Ni)$Ti_2$ compounds. Fig. 2c is the TEM image of interface between HEA phase and (Co, Ni)$Ti_2$ phase. The SAED patterns of HEA phase and (Co, Ni)$Ti_2$ compounds show that HEA phase along [001] zone axis confirms a B2 structure (Fig. 2e) and (Co, Ni)$Ti_2$ compounds along [011] zone axis confirms a FCC structure (Fig. 2f). From Fig. 2d, the interplanar spacing of BCC HEA phase is ~0.220 nm and the fast Fourier transform (FFT) image (Fig. 2g) of BCC HEA phase is in agreement with the SAED pattern (Fig. 2e). In a word, it can be deduced that the interface between BCC HEA phase and (Co, Ni)$Ti_2$ phase is incoherent or semi-coherent interface. As known to us, the incoherent or semi-coherent interface, which owns high interfacial energy, is easy to generate defects. Thus, the interface between BCC HEA phase and (Co, Ni)$Ti_2$ phase may be the initial failure place under the tensile force.

According to the process of tensile specimen preparation (Fig. 1), a large-scale dumbbell-shaped sample of approximate 4um × 700 nm × 90 nm (length × width × thickness) in observation region was obtained. Fig. 3 shows the TEM images and corresponding SAED images before and after tensile testing. From Fig. 3a, two obvious phases (marked 1 and 2, respectively) are shown and proved to be BCC HEA phase and (Co, Ni)$Ti_2$ phase, respectively, according to corresponding SAED images. That is, it agrees with the result of microstructure characterization [25]. Seen in Fig. 3b, it indicates the occurrence of the fracture phenomenon. The SAED image was gained near the area of fracture (white circle in Fig. 3b), which contains BCC HEA phase (blue quadrangle) and (Co, Ni)$Ti_2$ phase (red quadrangle). Referring to the yellow arrow in Fig. 3b, an interesting phenomenon, a diffraction ring occurs, can be clearly seen, which declares that amorphous phase is produced. For mechanical tests of materials with metallic bond carried out inside TEM, no obvious e-beam effect has been observed so far [17]. So the

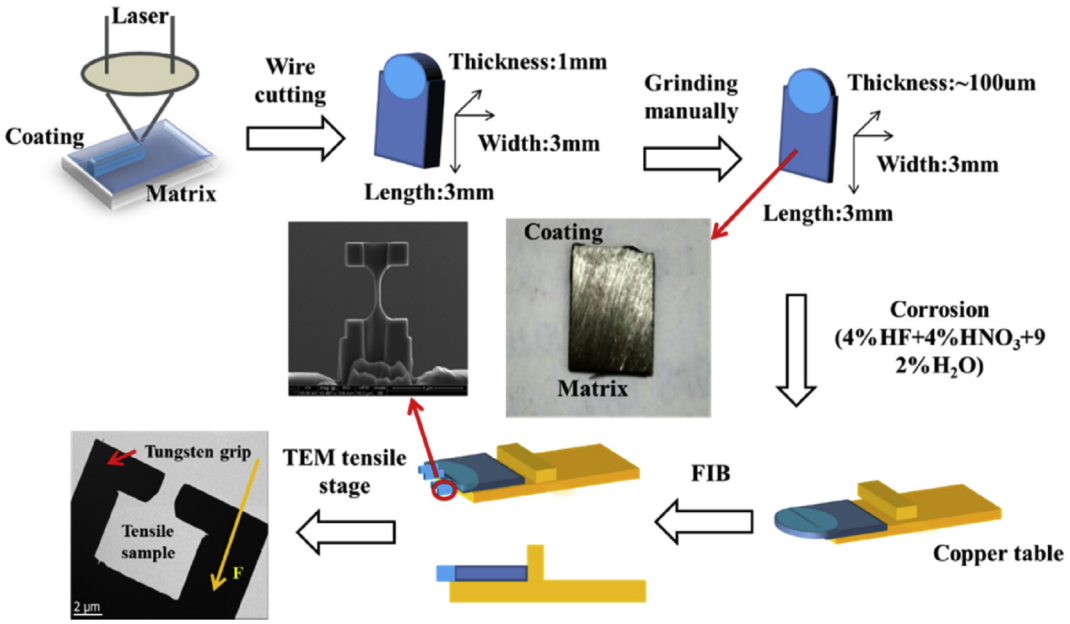


**Fig. 1.** Schematic diagram of tensile specimen preparation.

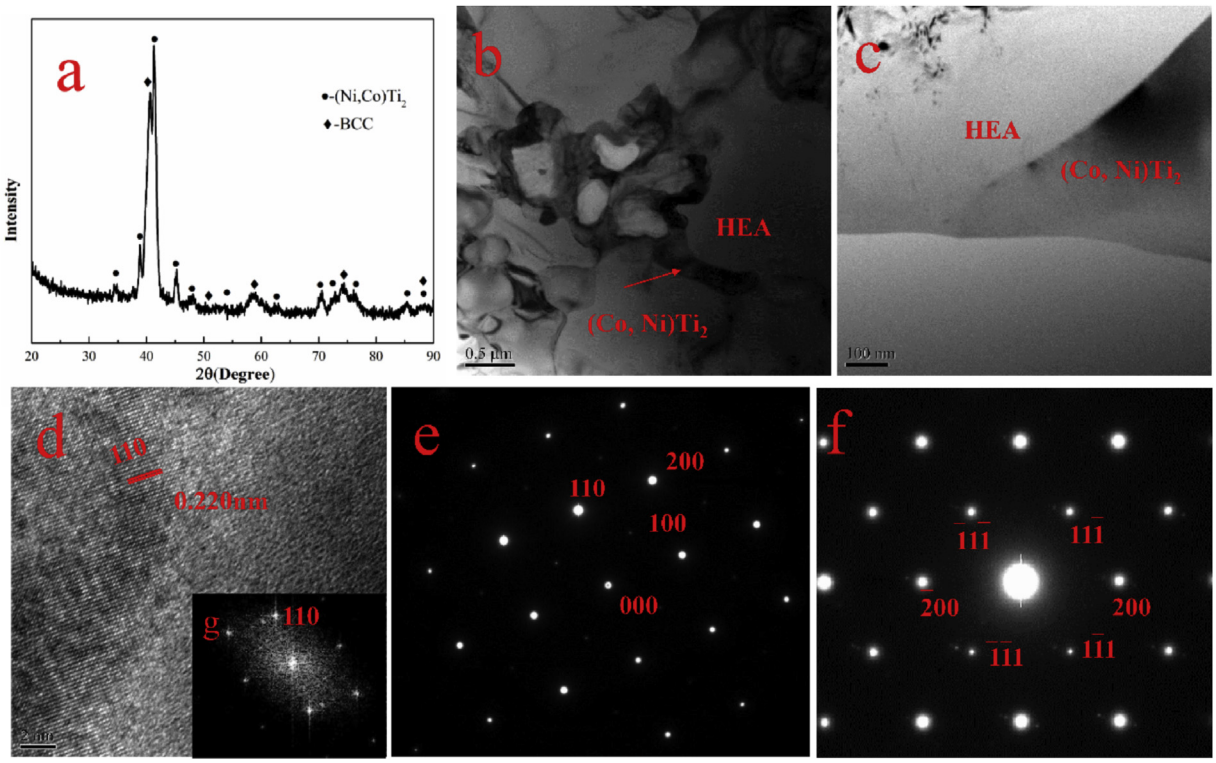


**Fig. 2.** XRD pattern of HEA coating (a); TEM images of complex HEA coating (b) and phase interface of BCC HEA/(Co, Ni)$Ti_2$ (c); HRTEM image of phase interface of BCC HEA/(Co, Ni)$Ti_2$ (d); SAED pattern of HEA phase(e) and (Co, Ni)$Ti_2$ phase (f); FFT image of HEA phase in Fig. 2d (g).

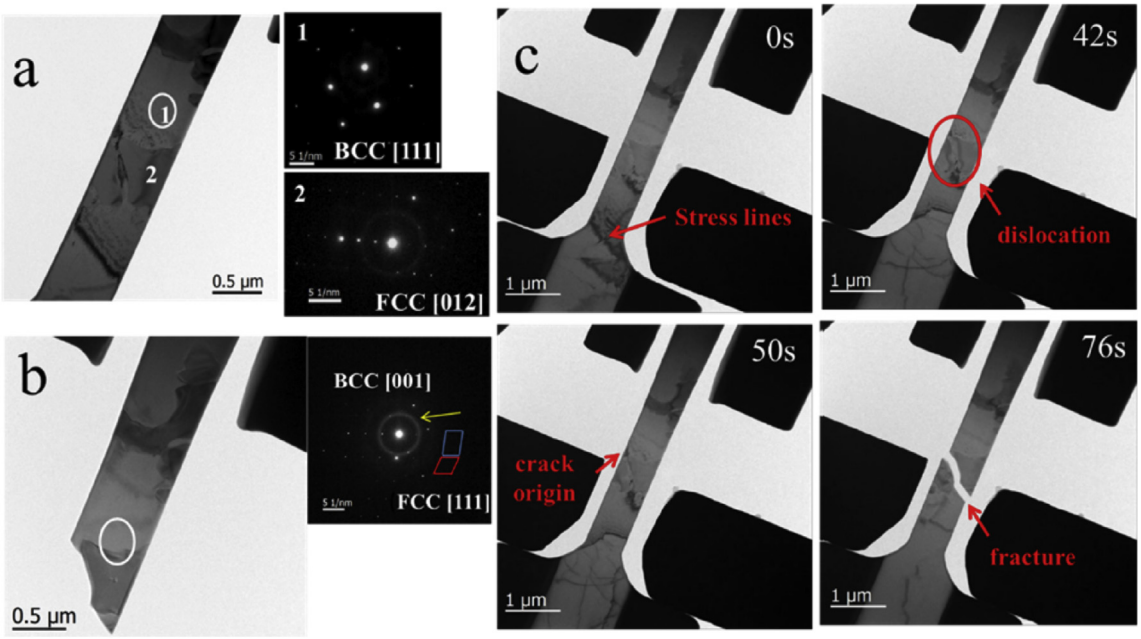


**Fig. 3.** (a) TEM images and corresponding SAED images before tensile testing; (b) TEM images and corresponding SAED images after tensile testing; (c) evolution of fracture process during *in situ* TEM tensile testing.

effect of e-beam could be excluded. Simultaneously, the crystal-to-amorphous transformation has been observed by experiments [26,27]. Thus, we can assume that the tensile stress during *in situ* TEM tensile testing induces the formation of amorphous phase. And the process of crystal-to-amorphous transformation is mainly due to dislocation accumulation [27]. Fig. 3c shows the evolution process of fracture in some certain time during *in situ* TEM tensile testing. The real sample evolution during the testing was recorded in a movie submitted in the supplementary material. From Fig. 3c, it is seen that the fracture process is slowly under way as time goes on. The stress lines, generated by the combined action of tensile stress and electron, are the most obvious change, that is, they flow

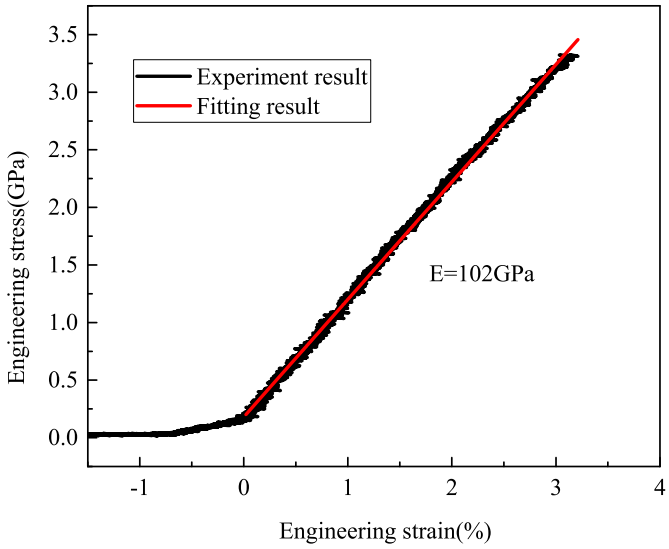


**Fig. 4.** Stress-strain curve from the *in situ* TEM tensile testing.

on the surface of the sample with loading force sustaining. When the time is 42s, the phenomenon of dislocations pile-up happens and dislocations get together in the interface of BCC HEA phase and (Co, Ni)$Ti_2$ phase, then they stimulate the nucleation of micro-cracks. Thus, the micro-crack origin forms at the time of 50s. Soon afterwards, the micro-crack origin expands along the phase interface unceasingly. In that case, the sample eventually fractures with the continuous tensile stress.

Fig. 4 exhibits the resulting stress-strain curve from the *in situ* TEM tensile testing. The curve shows a good linearity, namely, the stress increased with the strain nearly linearly until the abrupt fracture, confirming the brittle failure due to the absence of yield platform in the curve. Similar results have been observed in the visible or conventional tensile experiments [28,29], in which these composite coatings also belong to a brittle fracture without a yielding phenomenon. In our view, the major component of BCC HEA solid solution in the tensile sample, which has a relatively lower plasticity compared with FCC solid solution, may result in the brittle failure partly. Also, as indicated in Fig. 4, the fracture strength is calculated to be ~3.3 GPa and the fracture strain is measured to be ~3.1%. Therefore, according to linear fitting, the Young's modulus is calculated to be ~102 GPa, quite close to that of bulk titanium alloy. In general, the Young's modulus of material is not sensitive to variation of organization, cold plastic deformation and physical size, only depending on the physical properties of the material itself. So the Young's modulus of Ni-Cr-Co-Ti-V-Al HEA coating can be conceptually considered as ~102 GPa.

On the macro-scale, it is well known that the tensile failure can emerge in a brittle coating attached to a ductile substrate when it is subjected to the tensile load [2,28,29]. The grain boundaries, the interfaces between different phases and the brittle second phases may be three of the most vulnerable areas in the brittle coating with complex phases. Xu et al. [2] have proved that most of cracks are initiated from the brittle second phases (WC particles), and then propagated throughout the coating, which was attributed to the stress concentration in the brittle second phases (WC particles) or the areas near the brittle second phases (WC particles). Fan et al. [28] have displayed that the fracture mechanism of the Co-based coatings is mainly of an inter-granular nature and silicon carbide, boron carbide and impure elements that gather at the grain boundaries are prone to fracture. In our work, a conclusion can be drew that the interfaces between different phases may be the probable failure place when the fracture happens in the brittle coatings. The fracture process is described as follows: At an early stage of tensile testing, the coating resists the axial tensile force doggedly. Whereafter, owing to the differences of physical attribute between BCC HEA phase and (Co, Ni)$Ti_2$ phase, the stress starts to concentrate on the interface between different phases, proven by the result of finite element modelling in Fig. 5. With that, dislocations get together to hinder the concentration of stress. However, as the stress increases, the capacity of dislocations pile-up becomes saturated, as a result of stimulating the nucleation of micro-cracks. At the final stage of tensile testing, crack propagation happens along the interface between different phases, leading to rupture. This chain reaction is self-sustained and tends to localize very quickly in a given section of the sample, proving a brittle fracture assuredly.

In our work, the fracture strength of this HEA coating in *in situ* TEM observation is much higher than that of most reported HEAs and metallic alloys, which may be due to the high-entropy effect and the size effect. It is well known that the size-controlled

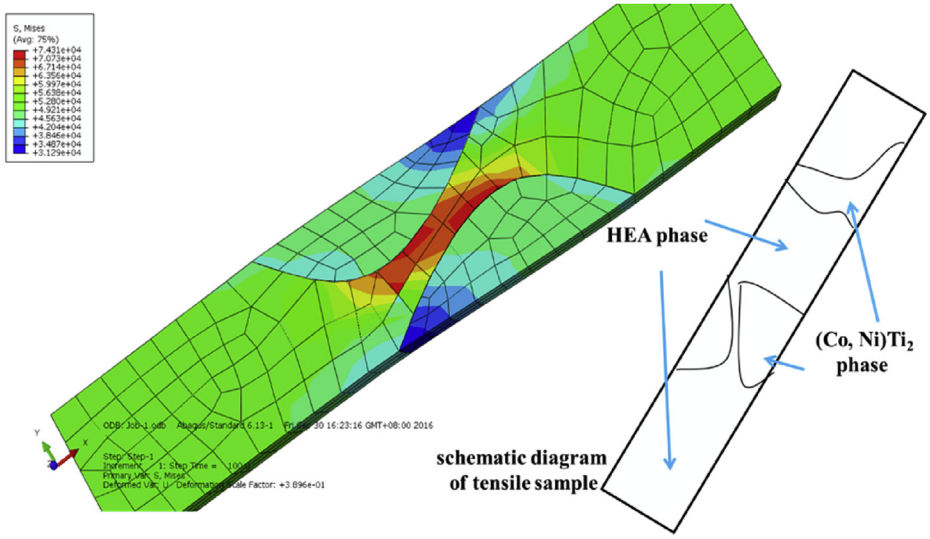


**Fig. 5.** Stress diagram of specific location of tensile sample.

macroscopic properties in *in situ* TEM observation could be different from that in macroscopic experiments, where individual grains are well surrounded and confined by the neighboring grains. In general, the ability of a material to resist fracture is proverbial defined as the combination of strength and toughness. However, in many traditional materials, especially metallic alloys, toughness comes at the expense of strength. Interestingly, HEAs usually possess a good compatibility of strength and toughness, showing an outstanding tensile properties [30,31].

## 4. Conclusions

We tentatively employed the *in situ* TEM tensile testing to study the fracture process of Ni-Cr-Co-Ti-V-Al HEA coating with complex phases. The novelty of this technique gives the ability to observe the whole fracture process in the brittle coating. The interfaces between different phases may be the probable failure point when the fracture happens. During the fracture process, dislocations pile-up happens in the interface between different phases and crack propagation happens along the interface, leading to final rupture. The stress-strain curve from the *in situ* TEM tensile testing shows a good linearity, confirming the brittle failure. From this curve, the fracture strength is calculated to be ~3.3 GPa and the fracture strain is measured to be ~3.1%. Therefore, the Young's modulus is calculated to be ~102 GPa.

## Acknowledgments

This work was financially supported by National Natural Science Foundation of China (No. 51375106, 51575118), National Basic Research Program of China (973 Program) (No. 61328303), China Postdoctoral Science Foundation (No. 2015M571390), Hei Long Jiang Postdoctoral Foundation (No. LBH-Z14050), Special Foundation for Harbin Science and Technology Innovation (No. 2015RAXXJ016) and Fundamental Research Funds for the Central Universities (No. HEUCFP2016154).

## References

[1] T. Wang, M. Zhang, W. Xiong, R. Liu, W. Shi, L. Li, Microstructure and tensile properties of the laser welded TWIP steel and the deformation behavior of the fusion zone, Mater. Des. 83 (2015) 103–111.
[2] J.S. Xu, X.C. Zhang, F.Z. Xuan, F.Q. Tian, Z.D. Wang, S.T. Tu, Tensile properties and fracture behavior of laser cladded WC/Ni composite coatings with different contents of WC particle studied by in-situ tensile testing, Mat. Sci. Eng. A 560 (2013) 744–751.
[3] F. Yang, R. Song, Y. Li, T. Sun, K. Wang, Tensile deformation of low density duplex Fe–Mn–Al–C steel, Mater. Des. 76 (2015) 32–39.
[4] B.H. An, I.T. Jeon, J.H. Seo, J.P. Ahn, O. Kraft, I.S. Choi, Y.K. Kim, Ultrahigh tensile strength nanowires with a Ni/Ni-Au multilayer nanocrystalline structure, Nano Lett. 16 (2016) 3500–3506.
[5] J.H. Seo, H.S. Park, Y. Yoo, T.Y. Seong, J. Li, J.P. Ahn, B. Kim, I.S. Choi, Origin of size dependency in coherent-twin-propagation-mediated tensile deformation of noble metal nanowires, Nano Lett. 13 (2013) 5112–5116.
[6] A.M. Minor, J.W. Morris, E.A. Stach, Quantitative in situ nanoindentation in an electron microscope, Appl. Phys. Lett. 79 (2001) 1625.
[7] Z. Shan, J.M.K. Wiezorek, J.A. Knapp, D.M. Follstaedt, E.A. Stach, S.X. Mao, Large lattice strain in individual grains of deformed nanocrystalline Ni, Appl. Phys. Lett. 92 (2008) 091917.
[8] Z. Shan, J.A. Knapp, D.M. Follstaedt, E.A. Stach, J.M. Wiezorek, S.X. Mao, Inter- and intra-agglomerate fracture in nanocrystalline nickel, Phys. Rev. Lett. 100 (2008) 105502.
[9] Z.W. Shan, R.K. Mishra, S.A. Syed Asif, O.L. Warren, A.M. Minor, Mechanical annealing and source-limited deformation in submicrometre-diameter Ni crystals, Nat. Mater. 7 (2008) 115–119.
[10] C. Chisholm, H. Bei, M.B. Lowry, J. Oh, S.A. Syed Asif, O.L. Warren, Z.W. Shan, E.P. George, A.M. Minor, Dislocation starvation and exhaustion hardening in Mo alloy nanofibers, Acta Mater. 60 (2012) 2258–2264.
[11] Q. Yu, Z.W. Shan, J. Li, X. Huang, L. Xiao, J. Sun, E. Ma, Strong crystal size effect on deformation twinning, Nature 463 (2010) 335–338.
[12] E. Hosseinian, O.N. Pierron, Quantitative in situ TEM tensile fatigue testing on nanocrystalline metallic ultrathin films, Nanoscale 5 (2013) 12532–12541.
[13] A.M. Minor, S.A. Asif, Z. Shan, E.A. Stach, E. Cyrankowski, T.J. Wyrobek, O.L. Warren, A new view of the onset of plasticity during the nanoindentation of aluminium, Nat. Mater. 5 (2006) 697–702.
[14] Z.W. Shan, J. Li, Y.Q. Cheng, A.M. Minor, S.A. Syed Asif, O.L. Warren, E. Ma, Plastic flow and failure resistance of metallic glass: insight fromin sit-ucompression of nanopillars, Phys. Rev. B 77 (2008) 155419.
[15] Q. Deng, Y. Cheng, Y. Yue, L. Zhang, Z. Zhang, X. Han, E. Ma, Uniform tensile elongation in framed submicron metallic glass specimen in the limit of suppressed shear banding, Acta Mater. 59 (2011) 6511–6518.
[16] L. Tian, Y.Q. Cheng, Z.W. Shan, J. Li, C.C. Wang, X.D. Han, J. Sun, E. Ma, Approaching the ideal elastic limit of metallic glasses, Nat. Commun. 3 (2012) 609.
[17] Z. Shan, In situ TEM investigation of the mechanical behavior of micro-nanoscaled metal pillars, Jom 64 (2012) 1229–1234.
[18] D.M. Tang, X.L. Wei, M.S. Wang, N. Kawamoto, Y. Bando, C.Y. Zhi, M. Mitome, A. Zak, R. Tenne, D. Golberg, Revealing the anomalous tensile properties of $WS_2$ nanotubes by in situ transmission electron microscopy, Nano Lett. 13 (2013) 1034–1040.
[19] H. Zheng, A. Cao, C.R. Weinberger, J.Y. Huang, K. Du, J. Wang, Y. Ma, Y. Xia, S.X. Mao, Discrete plasticity in sub-10-nm-sized gold crystals, Nat. Commun. 1 (2010) 144.
[20] J.W. Yeh, S.K. Chen, J.Y. Gan, S.J. Lin, T.S. Chin, T.T. Shun, C.H. Tsau, S.Y. Chang, Formation of simple crystal structures in Cu-Co-Ni-Cr-Al-Fe-Ti-V alloys with multiprincipal metallic elements, Metall. Mater. Trans. A 35A (2004) 2533–2536.
[21] J.W. Yeh, S.K. Chen, S.J. Lin, J.Y. Gan, T.S. Chin, T.T. Shun, C.H. Tsau, S.Y. Chang, Nanostructured high-entropy alloys with multiple principal elements: novel alloy design concepts and outcomes, Adv. Eng. Mater. 6 (2004) 299–303.
[22] Y. Zhang, T.T. Zuo, Z. Tang, M.C. Gao, K.A. Dahmen, P.K. Liaw, Z.P. Lu, Microstructures and properties of high-entropy alloys, Prog. Mater. Sci. 61 (2014) 1–93.
[23] Y. Wu, W.H. Liu, X.L. Wang, D. Ma, A.D. Stoica, T.G. Nieh, Z.B. He, Z.P. Lu, In-situ neutron diffraction study of deformation behavior of a multi-component high-entropy alloy, Appl. Phys. Lett. 104 (2014) 051910.
[24] Z. Zhang, M.M. Mao, J. Wang, B. Gludovatz, Z. Zhang, S.X. Mao, E.P. George, Q. Yu, R.O. Ritchie, Nanoscale origins of the damage tolerance of the high-entropy alloy CrMnFeCoNi, Nat. Commun. 6 (2015) 10143.
[25] Z. Cai, G. Jin, X. Cui, Z. Liu, W. Zheng, Y. Li, L. Wang, Synthesis and microstructure characterization of Ni-Cr-Co-Ti-V-Al high entropy alloy coating on Ti-6Al-4V substrate by laser surface alloying, Mater. Charact. 120 (2016) 229–233.
[26] C. Rentenberger, T. Waitz, H.P. Karnthaler, Formation and structures of bulk nanocrystalline intermetallic alloys studied by transmission electron microscopy, Mat. Sci. Eng. A 462 (2007) 283–288.
[27] J. Koike, D.M. Parkin, Crystal-to-amorphous transformation of NiTi induced by cold rolling, J. Mater. Sci. 5 (1990) 1414–1418.
[28] Y. Fan, G. Jin, X. Cui, Y. Li, Z. Gao, Effect of Nb and $CeO_2$ on the mechanical and tribology properties of Co-based cladding coatings, Surf. Coat. Technol. 288 (2016) 25–29.
[29] X. Duan, S. Gao, Q. Dong, Y. Zhou, M. Xi, X. Xian, B. Wang, Reinforcement mechanism and wear resistance of $Al_2O_3$/Fe-Cr-Mo steel composite coating produced by laser cladding, Surf. Coat. Technol. 291 (2016) 230–238.
[30] J.Y. He, H. Wang, H.L. Huang, X.D. Xu, M.W. Chen, Y. Wu, X.J. Liu, T.G. Nieh, K. An, Z.P. Lu, A precipitation-hardened high-entropy alloy with outstanding tensile properties, Acta Mater. 102 (2016) 187–196.
[31] Y.D. Wu, Y.H. Cai, T. Wang, J.J. Si, J. Zhu, Y.D. Wang, X.D. Hui, A refractory $Hf_{25}Nb_{25}Ti_{25}Zr_{25}$ high-entropy alloy with excellent structural stability and tensile properties, Mater. Lett. 130 (2014) 277–280.